Host (nanocavity of zeolite-Y)/guest ([Cu([R]$_2$-N$_2$X$_2$)]$^{2+}$ (R = H, CH$_3$; X = NH, O, S) nanocomposite materials: Synthesis, characterization and catalytic oxidation of ethylbenzene

Masoud Salavati-Niasari [a,b,∗]

[a] *Institute of Nano Science and Nano Technology, University of Kashan, Kashan, P.O. Box 87317-51167, Islamic Republic of Iran*
[b] *Department of Chemistry, Faculty of Science, University of Kashan, Kashan, P.O. Box 87317-51167, Islamic Republic of Iran*

Abstract

Copper(II) complexes of 12-membered macrocyclic ligands having three different donating atoms (N$_2$O$_2$, N$_2$S$_2$ and N$_4$) in the macrocyclic ring have been encapsulated in the nanocavity of zeolite-Y by the fexible-ligand method. Copper(II) complexes with macrocyclic ligands were entrapped in the nanocavity of zeolite-Y by a two-step process in the liquid phase: (i) adsorption of precursor ligand; 1,2-di(*o*-aminophenyl-, amino, oxo, thio)ethane, N$_2$X$_2$; in the supercages of the Cu(II)–NaY, and (ii) in situ condensation of the Cu(II) precursor complex; [Cu(N$_2$X$_2$)]$^{2+}$; with glyoxal or biacetyl. The new host–guest nanocomposite materials (HGNM); [Cu([R]$_2$-N$_2$X$_2$)]$^{2+}$–NaY (R = H, CH$_3$; X = NH, O, S); have been characterized by FT-IR, DRS and UV–vis spectroscopic techniques, XRD and elemental analysis, as well as nitrogen adsorption. The "neat" and encapsulated complexes exhibited good catalytic activity in the oxidation of ethylbenzene at 333 K, using *tert*-butylhydroperoxide (TBHP) as the oxidant. Acetophenone was the major product though small amounts of *o*- and *p*-hydroxyacetophenones were also formed revealing that C−H bond activation takes place both at benzylic and aromatic ring carbon atoms. Ring hydroxylation was more over the "neat" complexes than over the encapsulated complexes.

1. Introduction

Encapsulation of transition metal complexes within nanocavity of zeolite-Y (host–guest nanocomposite materials; HGNM) has emerged as a general technique to increase and control selectivity of catalysts [1]. In addition, the confinement of guest molecules leads to a higher stability by reducing dimerization of active sites. Nanopores of zeolite-Y are attractive hosts for encapsulation as they combine a high thermal and chemical stability with a quite regular, crystalline framework structure. Zeolite complexes posses a number of structural similarities to metalloenzymes and therefore they are expected to mimic enzyme active sites for the catalytic reaction. They are known to catalyze a variety of reactions such as oxidation, hydrogenation, dehalogenation, Friedel–Crafts alkylation and alkylaromatic isomerization or disproportionation, etc. [2–13]. The heterogenization of homogenous catalysts due to the site isolation effect is a field of continuing interest. Although some of homogeneous transition metal complexes exhibit remarkable catalytic properties (activities and selectivity), they are unsuitable to separate intact from the reaction medium making their reuse difficult and contaminating the reaction products. Thus, the heterogenization is always a toxicological and environmental challenge; moreover, it has an economical significance unless the activities of the neat catalysts are exceptionally high.

Zeolites, which represent the largest group of nanoporous materials, are crystalline inorganic polymers based on a three-dimensional arrangement of SiO$_4$ and AlO$_4$ tetrahedra connected through their oxygen atoms to form large negatively charged lattices with Brönsted and Lewis acid sites. These negative charges are balanced by extra-framework alkali and/or alkali earth cations. The incorporation of small amounts of transition

─────────

∗ Correspondence address: Institute of Nano Science and Nano Technology, University of Kashan, Kashan, P.O. Box 87317-51167, Islamic Republic of Iran. Tel.: +98 361 5555 333; fax: +98 361 555 29 30.

E-mail address: salavati@kashanu.ac.ir.

metals into zeolitic frameworks influences their properties and generates their redox activity. Zeolites with their well-organized and regular system of nanopores and nanocavities also represent almost ideal matrices for hosting nanosized particles, e.g., transition metal complexes that can also be involved in catalytic applications.
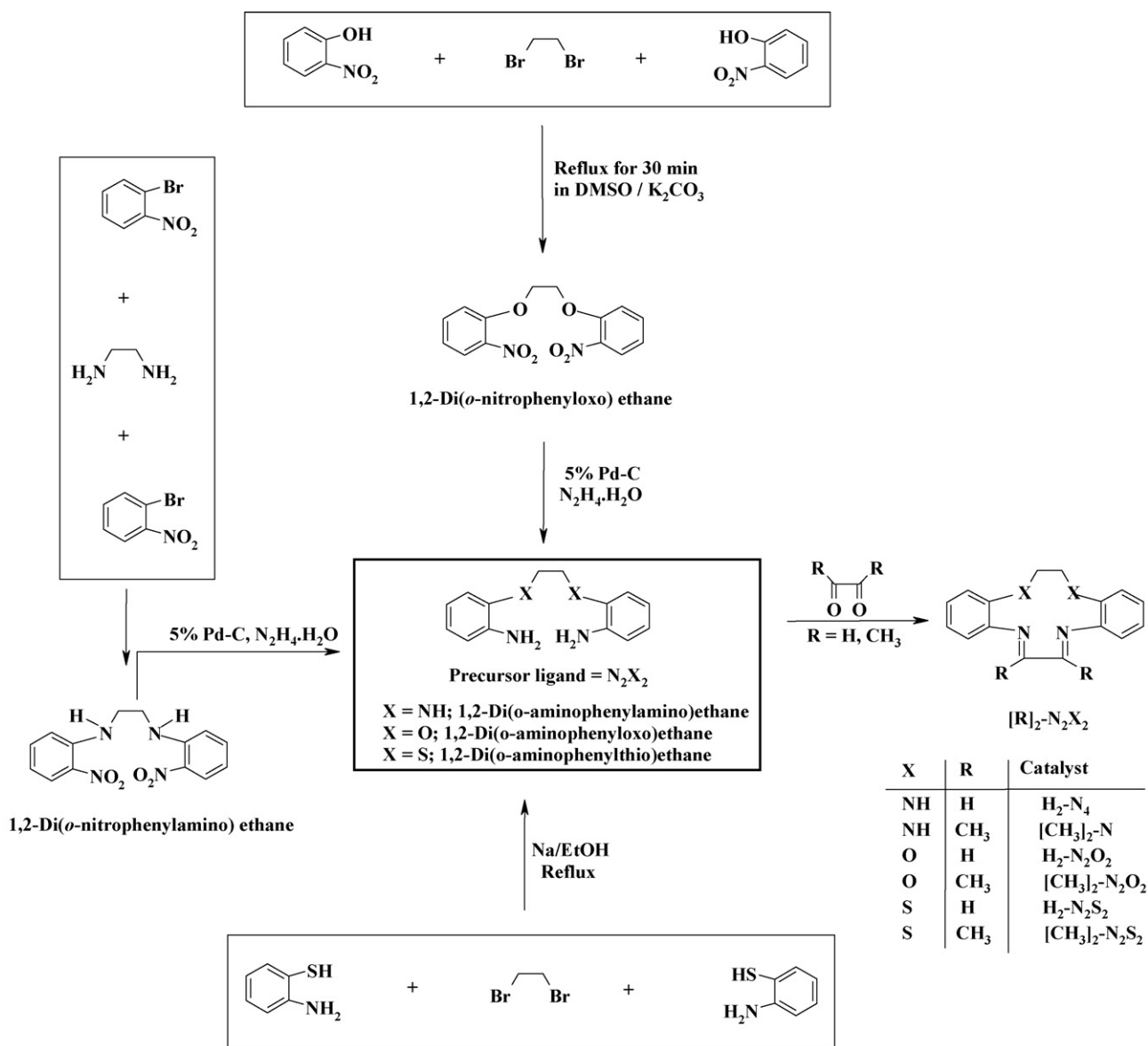
In this paper, the synthesis and characterization of copper(II) complexes of 12-membered macrocyclic ligand; 1,4-diaza,7,10-dioxo,5,6:11,12-dibenzo-[e,k]-cyclododeca-1,3-diene[N$_2$O$_2$]ane; [H]$_2$-N$_2$O$_2$, 2,3-dimethyl-1,4-diaza,7,10-dioxo,5,6:11,12-dibenzo-[e,k]-cyclododeca-1,3-diene[N$_2$O$_2$]ane; [CH$_3$]$_2$-N$_2$O$_2$, 1,4,7,10-tetraaza-5,6:11,12-dibenzo-[e,k]-cyclododeca-1,3-diene[N$_4$]ane; [H]$_2$-N$_4$, 2,3-dimethyl-1,4,7,10-tetraaza-5,6:11,12-dibenzo-[e,k]-cyclododeca-1,3-diene[N$_4$]ane; [CH$_3$]$_2$-N$_4$, 1,4-diaza,7,10-dithia,5,6:11,12-dibenzo-[e,k]-cyclododeca-1,3-diene[N$_2$S$_2$]ane; [H]$_2$-N$_2$S$_2$) and 2,3-dimethyl-1,4-diaza,7,10-dithia,5,6:11,12-dibenzo-[e,k]-cyclododeca-1,3-diene[N$_2$S$_2$]ane; [CH$_3$]$_2$-N$_2$S$_2$; encapsulated within the nanopores of zeolite-Y by the template condensation of glyoxal or biacetyl and precursor complex ([Cu([R]$_2$-N$_2$X$_2$)]$^{2+}$–NaY, R = H, CH$_3$; X = NH, O, S), Schemes 1 and 2, reported. These complexes were used in the oxidation of ethylbenzene with *tert*-butylhydroperoxide (TBHP) as oxygen donor.
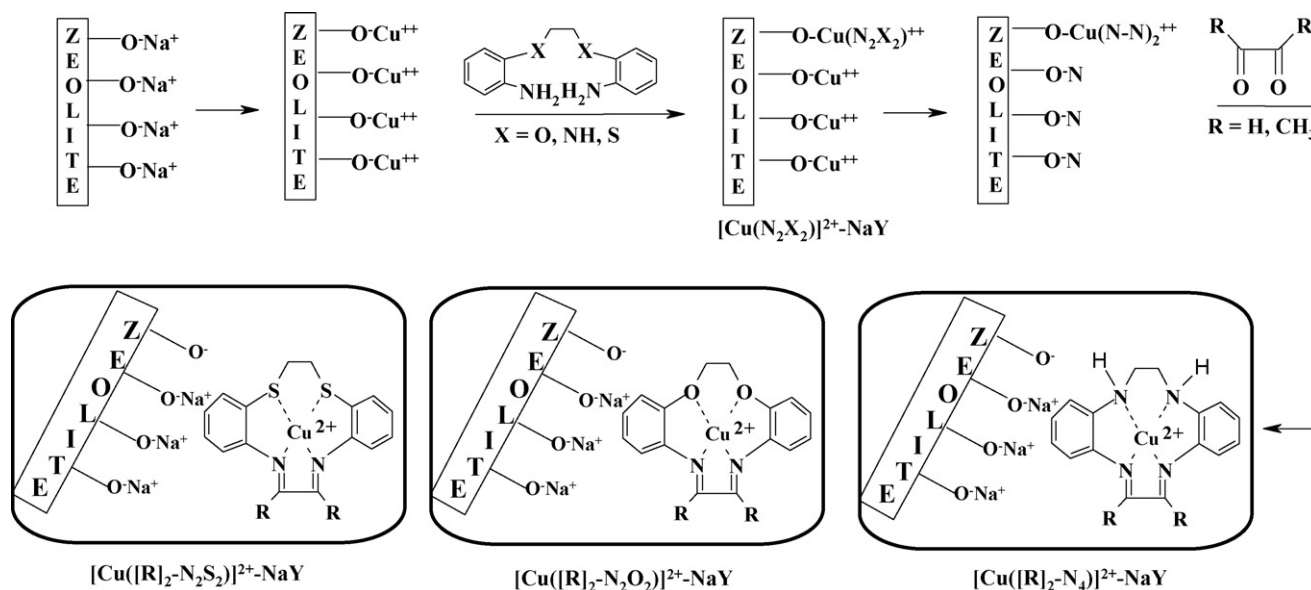
2. Experimental

2.1. Materials and physical measurements

All other reagents and solvent were purchased from Merck (pro-analysis) and dried using molecular sieves (Linde 4 Å). *Tert*-butlhydroperoxide; TBHP; (solution 50% in ethylenedichloride), glyoxal and biacetyl were obtained from Merck Co. NaY with the Si:Al ratio of 2.53 was purchased

X	R	Catalyst
NH	H	H$_2$-N$_4$
NH	CH$_3$	[CH$_3$]$_2$-N
O	H	H$_2$-N$_2$O$_2$
O	CH$_3$	[CH$_3$]$_2$-N$_2$O$_2$
S	H	H$_2$-N$_2$S$_2$
S	CH$_3$	[CH$_3$]$_2$-N$_2$S$_2$

Scheme 1. Reaction mechanism of 12-membered macroccyclic ligands.

Scheme 2.

from Aldrich (lot no. 67812). FT-IR spectra were recorded on Shimadzu Varian 4300 spectrophotometer in KBr pellets. The electronic spectra of the neat complexes were taken on a Shimadzu UV–vis scanning spectrometer (Model 2101 PC). Diffuse reflectance spectra (DRS) were registered on a Shimadzu UV/3101 PC spectrophotometer the range 1500–200 nm, using MgO as reference. The elemental analysis (carbon, hydrogen and nitrogen) of the materials was obtained from Carlo ERBA Model EA 1108 analyzer. XRD patterns were recorded by a Rigaku D-max C III, X-ray diffractometer using Ni-filtered Cu Kα radiation. Nitrogen adsorption measurements were performed at 77 K using a Coulter Ofeisorb 100CX instrument. The samples were degassed at 150 °C until a vacuum better than 10^{-3} Pa was obtained. Micropore volumes were determined by the *t*-method, a "monolayer equivalent area" was calculated from the micropore volume [14,15]. The stability of the encapsulated catalyst was checked after the reaction by UV–vis and possible leaching of the complex was investigated by UV–vis in the reaction solution after filtration of the zeolite. The amounts of copper(II) metallocomplexes encapsulated in zeolite matrix were determined by the elemental analysis and by subtracting the amount of copper(II) complex left in the solutions after the synthesis of the catalysts as determined by UV–vis spectroscopy, from the amount taken for the synthesis. Atomic absorption spectra (AAS) were recorded on a Perkin Elmer 4100–1319 Spectrophotometer using a flame approach, after acid (HF) dissolution of known amounts of the zeolitic material and SiO_2 was determined by gravimetric analysis.

2.2. Synthesis of 1,2-di(o-aminophenyloxo)ethane

Ortho-nitrophenol (4.78 g) in hot dimethylformamide (5.0 ml) was treated slowly with potassium carbonate (2.39 g). The resulting solution was boiled gently and 1,2-dibromoethane (1.54 ml) was added dropwise with constant stirring for 30 min. The mixture was then refluxed for 2 h and concentrated under reduced pressure. On pouring the solution into cold water a granular yellow solid was filtered, washed with dilute aqueous NaOH, dried and recystallized from glacial acetic acid, M.P. 169 °C, ^{1}H NMR: (CDCl₃) δ 8.18 (2H, d), δ 7.35 (2H, m), δ 7.76 (2H, m), δ 7.08 (H, d), δ 4.08 (4H, O-CH₂) (Scheme 1).

1,2-Di(*o*-nitrophenyloxo)ethane was heated under a nitrogen atmosphere with 5% Pd-C (0.5 g). $N_2H_4·H_2O$ (20.0 ml) was added in (5 ml) portions and the mixture refluxed until the solution become colorless (30 min). After filtration to remove the precipitate (if any), the solution was evaporated to dryness and the solid residue recrystallized from hot ethanol under a nitrogen atmosphere. A residue of white plates was obtained. M.P. 131 °C. ^{1}H NMR: (CDCl₃) δ 6.35 (2H, d), δ 7.16 (2H, m), δ 6.65 (2H, m), δ 7.08 (2H, d), δ 4.03 (4H, O-CH₂) (Scheme 1).

2.3. Synthesis of 1,2-di(o-aminophenylamino)ethane

1,2-Di(*o*-nitrophenylamino)ethane was prepared by heating $BrC_6H_4NO_2$ (2.0 g) with 1,2-diaminoethane (0.26 ml). The mixture was stirred rigorously until complete reaction had occurred. The heating was then reduced to keep the mass molten for a further use. The melt was poured into ethanol (50.0 ml), the solid so obtained was washed with a mixture of diethyl ether (30.0 ml), benzene (30.0 ml) and 1N NaOMe solution (10 ml). It was recrystallized from 1,2-dichloroethane give 1,2-di(*o*-nitrophenylamino)ethane (3.1 g) as bright orange needle shaped crystals. M.P. 193 °C. ^{1}H NMR: (CDCl₃) δ 8.1 (2H, d), δ 7.33 (2H, m), δ 7.75 (2H, m), δ 7.06 (H, d), δ 4.07 (4H, NH-CH₂) (Scheme 1).

1,2-Di(*o*-nitrophenylamino)ethane was heated under a nitrogen atmosphere with 5% Pd-C (0.5 g). $N_2H_4·H_2O$ (20.0 ml) was added in (5 ml) portions and the mixture refluxed until the solu-

tion become colorless (30 min). After filtration to remove the precipitate (if any), the solution was evaporated to dryness and the solid residue recrystallized from hot ethanol under a nitrogen atmosphere. A residue of white plates was obtained. M.P. 135 °C. ^{1}H NMR: (CDCl$_3$) δ 6.36 (2H, d), δ 7.15 (2H, m), δ 6.65 (2H, d), δ 6.73 (2H, d), δ 3.04 (4H, m, NH-CH$_2$) diamine(II) (Scheme 1).

2.4. Synthesis of 1,2-di(o-aminophenylthio)ethane

This diamine was prepared by heating o-HSC$_6$H$_4$NH$_2$ (1.09 g) with absolute (99%) ethanol (3 ml) containing sodium (0.201 g). 1,2-Dibromoethane (0.372 ml) in ethanol (1 ml) was added dropwise with constant stirring to the refluxing solution. The mixture was cooled and poured into water (300 ml). The solid mass so obtained, was filtered washed with water and dried. The product was recrystallized from ethanol, and a yellowish residue was obtained. M.P. 75 °C. ^{1}H NMR: (CDCl$_3$) δ 6.35 (2H, d), δ 7.15 (2H, m), δ 6.63 (2H, m), δ 7.24 (2H, d), δ 2.88 (4H, m, S-CH$_2$) (Scheme 1).

2.5. Synthesis of macrocyclic ligands ([R]$_2$-N$_2$X$_2$, R = H, CH$_3$; X = NH, O, S)

1,4-Diaza,7,10-dioxo,5,6:11,12-dibenzo-[e,k]-cyclododeca-1,3-diene[N$_2$O$_2$]ane; [H]$_2$-N$_2$O$_2$, 2,3-dimethyl-1,4-diaza,7,10-dioxo,5,6:11,12-dibenzo-[e,k]-cyclododeca-1,3-diene[N$_2$O$_2$] ane; [CH$_3$]$_2$-N$_2$O$_2$, 1,4,7,10-tetraaza-5,6:11,12-dibenzo-[e,k]-cyclododeca-1,3-diene[N$_4$]ane; [H]$_2$-N$_4$, 2,3-dimethyl-1,4,7,10-tetraaza-5,6:11,12-dibenzo-[e,k]-cyclododeca-1,3-diene[N$_4$]ane; [CH$_3$]$_2$-N$_4$, 1,4-diaza,7,10-dithia,5,6:11,12-dibenzo-[e,k]-cyclododeca-1,3-diene[N$_2$S$_2$]ane; [H]$_2$-N$_2$S$_2$ and 2,3-dimethyl-1,4-diaza,7,10-dithia,5,6:11,12-dibenzo-[e,k]-cyclododeca-1,3-diene[N$_2$S$_2$]ane; [CH$_3$]$_2$-N$_2$S$_2$ were obtained as described. To an ethanol solution (25 ml) of 0.05 mol glyoxal or biacetyl, an ethanol solution (25 ml) of precursor ligand; 1,2-di(o-aminophenyloxo)ethane, 1,2-di(o-aminophenylamino)ethane, 1,2-di(o-aminophenylthio)ethane (0.05 mol); was added in the presence of a few drops of conc. HCl and the resulting solution boiled under reflux for 8 h. The solution was then concentrated to half its volume under reduced pressure and kept overnight. The white/white off crystals which formed were filtered, washed with ethanol and dried under vacuum over P$_4$O$_{10}$. ^{1}H NMR, (CDCl$_3$); [H]$_2$-N$_4$: δ 8.01 (2H, s), 6.93 (2H, d), d 7.14 (2H, m), 6.65 (2H, m), 6.76 (2H, d), 3.12 (4H, NH-CH$_2$); [CH$_3$]$_2$-N$_4$: δ 2.09 (6H, s), 6.92 (2H, d), d 7.13 (2H, m), 6.65 (2H, m), 6.75 (2H, d), 3.11 (4H, NH-CH$_2$); [H]$_2$-N$_2$O$_2$: δ 8.05 (2H, s), 6.92 (2H, d), d 7.12 (2H, m), 6.63 (2H, m), 6.74 (2H, d), 4.13 (4H, O-CH$_2$); [CH$_3$]$_2$-N$_2$O$_2$: δ 2.13 (6H, s), 6.91 (2H, d), d 7.12 (2H, m), 6.62 (2H, m), 6.73 (2H, d), 4.13 (4H, O-CH$_2$); [H$_2$]-N$_2$S$_2$: δ 7.92 (2H, s), 6.90 (2H, d), d 7.11 (2H, m), 6.60 (2H, m), 6.72 (2H, d), 4.11 (4H, S-CH$_2$); [CH$_3$]$_2$-N$_2$S$_2$: δ 1.94 (6H, s), 6.90 (2H, d), d 7.10 (2H, m), 6.60 (2H, m), 6.72 (2H, d), 4.10 (4H, S-CH$_2$) (Scheme 1).

2.6. Preparation of [Cu([R]$_2$-N$_2$X$_2$)](ClO$_4$)$_2$ (R = H, CH$_3$; X = NH, O, S)

Copper(II) sulfate pentahydrate (2.50 g, 0.01 mol) dissolved in ethanol (20 ml) was reacted with an ethanol (20 ml) solution 0.01 mol of 12-membered macrocyclic ligand ([H]$_2$-N$_4$, [CH$_3$]$_2$-N$_4$, [H]$_2$-N$_2$O$_2$, [CH$_3$]$_2$-N$_2$O$_2$, [H]$_2$-N$_2$S$_2$, [CH$_3$]$_2$-N$_2$S$_2$) by refluxing for 1 h under nitrogen atmosphere. The mixture was heated at reflux for 6 h until a yellow solution resulted. The solution was cooled to room temperature and filtered to remove copper hydroxide. Excess lithium perchlorate dissolved in methanol was added to the filtrate, and the mixture was kept in the refrigerator until yellow solid formed. The solids were filtered, washed thoroughly with cold ethanol and dried in vacuum.

2.7. Preparation of [Cu(N$_2$X$_2$)]$^{2+}$–NaY (X = NH, O, S)

An amount of 5.0 g of Na-Y-zeolite was suspended in 300 ml distilled water, which contained copper(II) nitrate (50 mmol). The mixture was then heated with stirring at 90 °C for 24 h. The solid was filtered, washed with hot distilled water till the filtrate was free from any copper ion content, and dried for 12 h at 150 °C in air. The ionic exchange degree was determined by atomic absorption spectrophotometer. To a stirred methanol solution of Cu(II)–NaY (4 g) was added was uniformly mixed with an excessive amount of 1,2-di(o-aminophenyloxo)ethane, 1,2-di(o-aminophenylamino)ethane or 1,2-di(o-aminophenylthio)ethane ligands ($n_{ligand}/n_{metal} = 3$), and sealed into a round flask. The complexation was carried out under high vacuum conditions for 24 h at the temperatures of 150 °C. Uncomplexed ligands and the complex adsorbed on the exterior surface were removed by full Soxhlet extraction with ethanol. The extracted sample was ion-exchanged with 0.1 M NaCl aqueous solution to remove uncoordinated Cu^{2+} ions, followed by washing with deionized water until no Cl$^-$ anions could be detected with AgNO$_3$ aqueous solution.

2.8. Preparation of [Cu([R]$_2$-N$_2$X$_2$)]$^{2+}$–NaY (R = H, CH$_3$; X = NH, O, S)

To a stirred methanol suspension (100 ml) of precursor nanocatalyst ([Cu(N$_2$X$_2$)]$^{2+}$–NaY); (2 g) was slowly added glyoxal or biacetyl (under N$_2$ atmosphere). The mixture was heated under reflux condition for 24 h until a pale yellow suspension resulted. The solution was filtered and the resulting zeolites, were Soxhlet extracted with N,N'-dimethylformamide (for 4 h) and then with ethanol (for 4 h) to remove excess unreacted products from amine-carbonyl condensation and any copper(II) complexes adsorbed onto the external surface of the zeolite crystallites. The resulting pale yellow solids were dried at 70 °C under vacuum for 12 h. The remaining precursor ions in zeolite were removed by exchanging with aqueous 0.1 M NaNO$_3$ solutions. The stability of the encapsulated catalyst was checked after the reaction by UV–vis and possible leaching of the complex was investigated by UV–vis in the reaction solution after filtration of the zeolite. The amounts of Cu(II) complexes encapsulated in

Table 1
Elemental analysis, vibrations parameters and some physical properties for ligands and 12-membered macrocyclic copper(II) complexes

Complex	Calculated (found)					$\Lambda_M{}^a$, (Ω^{-1} cm^2 mol^{-1})	μ_{ef} (MB)	IR (KBr, cm^{-1})		$d \leftrightarrow d$ (nm)^a
	C (%)	H (%)	N (%)	C/N	Cu (%)			$\nu_{C=N}$	ν_{N-H}	
[H]$_2$-N$_4$	72.70 (72.58)	6.10 (5.93)	21.20 (21.34)	3.43 (3.40)	–	–	–	1620	3310	–
[CH$_3$]$_2$-N$_4$	73.94 (73.79)	6.90 (6.79)	19.16 (19.28)	3.86 (3.83)	–	–	–	1618	3300	–
[H]$_2$-N$_2$O$_2$	72.16 (72.01)	5.30 (5.18)	10.52 (10.70)	6.86 (6.73)	–	–	–	1615	–	–
[CH$_3$]$_2$-N$_2$O$_2$	73.45 (73.28)	6.16 (6.04)	9.52 (9.66)	7.72 (7.59)	–	–	–	1613	–	–
[H]$_2$-N$_2$S$_2$	64.14 (64.00)	4.71 (4.59)	9.35 (9.50)	6.86 (6.74)	–	–	–	1605	–	–
[CH$_3$]$_2$-N$_2$S$_2$	65.98 (65.76)	5.54 (5.40)	8.55 (8.69)	7.72 (7.72)	–	–	–	1602	–	–
[Cu([H]$_2$-N$_4$)](ClO$_4$)$_2$	36.48 (36.30)	3.06 (2.91)	10.64 (10.76)	3.43 (3.37)	12.06 (11.88)	260	1.73	1597	3285	485, 557
[Cu([CH$_3$]$_2$-N$_4$)](ClO$_4$)$_2$	38.97 (38.76)	3.63 (3.50)	10.10 (10.27)	3.86 (3.77)	11.45 (11.23)	249	1.72	1595	3280	484, 556
[Cu([H]$_2$-N$_2$O$_2$)](ClO$_4$)$_2$	36.35 (36.13)	2.67 (2.58)	5.30 (5.44)	6.86 (6.64)	12.02 (11.89)	255	1.73	1590	–	486, 555
[Cu([CH$_3$]$_2$-N$_2$O$_2$)](ClO$_4$)$_2$	38.83 (38.62)	3.26 (3.11)	5.03 (5.27)	7.72 (7.33)	11.41 (11.25)	245	1.71	1587	–	485, 554
[Cu([H]$_2$-N$_2$S$_2$)](ClO$_4$)$_2$	34.19 (34.01)	2.51 (2.33)	4.98 (5.11)	6.86 (6.65)	11.31 (11.17)	250	1.72	1586	–	487, 559
[Cu([CH$_3$]$_2$-N$_2$S$_2$)](ClO$_4$)$_2$	36.64 (36.45)	3.07 (2.89)	4.75 (4.90)	7.72 (7.44)	10.77 (10.51)	240	1.74	1583	–	488, 560

^{a} In acetonitrile solutions.

zeolite matrix were determined by the elemental analysis and by subtracting the amount of Cu(II) complex left in the solutions after the synthesis of the catalysts as determined by UV–vis spectroscopy, from the amount taken for the synthesis.

2.9. Oxidation of ethylbenzene; general procedure

The catalytic activity runs were conducted in a 25 ml glass round bottom flask placed in a thermostated oil bath and fitted with water cooled condenser. In a typical oxidation, ethylbenzene (0.106 g; 1 mmol), catalyst (0.004 mmol in case of "neat" complexes and 0.004 mmol in case of encapsulated complexes), TBHP (50% in ethylenedichloride; 0.42 ml) and CH$_3$CN (1 ml) were taken and the reaction was conducted at 333 K for 10 h. The progress of the reaction was monitored by GC and the products were identified by GC–MS.

3. Results and discussion

The synthesis of [Cu([R]$_2$-N$_2$X$_2$)]$^{2+}$ (R = H, CH$_3$; X = NH, O, S) encapsulated in the nanopores of zeolite-Y was carried out by the flexible ligand method as described by Ratnasamy and co-workers [16]. The crude mass was subjected to Soxhlet extraction in methanol to remove excess ligand that remained uncomplexed in the nanocavities of the zeolite as well as located on the surface of the zeolite along with free [Cu([R]$_2$-N$_2$X$_2$)]$^{2+}$, if any. The uncomplexed copper(II) ions from the zeolite was removed by exchanging back [Cu([R]$_2$-N$_2$X$_2$)]$^{2+}$–NaY with aqueous 0.01 M NaCl solution. Thus, presence of 0.638% of copper(II) estimated by atomic absorption spectrometer is only due to encapsulation of the complex. The resulting catalyst was further characterized by recording its IR and electronic spectra and X-ray powder diffraction (vide infra) pattern. All these studies further supported the encapsulation of [Cu([R]$_2$-N$_2$X$_2$)]$^{2+}$ inside the super cages of the zeolite. Neat complexes has also been prepared by the reaction of 12-membered macrocyclic ligands (1,4-diaza,7,10-dioxo,5,6:11,12-dibenzo-[e,k]-cyclododeca-1,3-diene[N$_2$O$_2$]ane; [H]$_2$-N$_2$O$_2$, 2,3-dimethyl-1,4-diaza,7,10-dioxo,5,6:11,12-dibenzo-[e,k]-cyclododeca-1,3-diene[N$_2$O$_2$]ane; [CH$_3$]$_2$-N$_2$O$_2$, 1,4,7,10-tetraaza-5,6:11,12-dibenzo-[e,k]-cyclododeca-1,3-diene[N$_4$]ane; [H]$_2$-N$_4$, 2,3-dimethyl-1,4,7,10-tetraaza-5,6:11,12-dibenzo-[e,k]-cyclododeca-1,3-diene[N$_4$]ane; [CH$_3$]$_2$-N$_4$, 1,4-diaza,7,10-dithia,5,6:11,12-dibenzo-[e,k]-cyclododeca-1,3-diene[N$_2$S$_2$]ane; [H]$_2$-N$_2$S$_2$) and 2,3-dimethyl-1,4-diaza,7,10-dithia,5,6:11,12-dibenzo-[e,k]-cyclododeca-1,3-diene[N$_2$S$_2$]ane; [CH$_3$]$_2$-N$_2$S$_2$) in presence of LiClO$_4$ with Cu(II) in refluxing methanol to yield the cationic complexes; [Cu([R]$_2$-N$_2$X$_2$)](ClO$_4$)$_2$, R = H, CH$_3$; X = NH, O, S; (Scheme 1). Acetonitrile solutions of these complexes were conductive (Table 1). Unfortunately, I could not grow any single crystals suitable for X-ray crystallographic studies. The molar conductance values of tetraaza macrocyclic complexes (240–260 Ω^{-1} mol^{-1} cm^2) and measured correspond to 1:2 electrolytes.

The chemical compositions confirmed the purity and stoichiometry of the neat and encapsulated complexes. The chemical analysis of the samples revealed the presence of organic matter

Table 2
Chemical composition and IR stretching frequencies (as KBr pellets) of nanopores of zeolite-encapsulated 12-membered macrocyclic copper(II) complexes

Sample	C (%)	H (%)	N (%)	C/N	Si (%)	Al (%)	Na (%)	Cu (%)	Si/Al	$\upsilon_{C=N}$ (cm^{-1})	$d \leftrightarrow d$ (nm)[a]
NaY	–	–	–	–	21.76	8.60	7.50	–	2.53	–	–
Cu(II)–NaY	–	–	–	–	21.48	8.49	3.28	3.86	2.53	–	–
$[Cu([H]_2-N_4)]^{2+}$–NaY	5.95	3.06	1.75	3.20	20.98	8.29	5.27	2.82	2.53	1595	556
$[Cu([CH_3]_2-N_4)]^{2+}$–NaY	5.66	3.13	1.60	3.56	20.94	8.28	5.26	2.80	2.53	1593	555
$[Cu([H]_2-N_2O_2)]^{2+}$–NaY	5.56	3.08	0.85	6.51	21.04	8.32	5.26	2.83	2.53	1590	553
$[Cu([CH_3]_2-N_2O_2)]^{2+}$–NaY	5.60	3.04	0.75	7.48	21.01	8.30	5.29	2.81	2.53	1585	552
$[Cu([H]_2-N_2S_2)]^{2+}$–NaY	5.52	3.00	0.83	6.64	20.93	8.27	5.27	2.79	2.53	1584	557
$[Cu([CH_3]_2-N_2S_2)]^{2+}$–NaY	5.54	3.05	0.74	7.46	20.90	8.26	5.25	2.77	2.53	1580	558

with a C/N ratio roughly similar to that for neat complexes. The percentage of copper(II) contents estimated before and after encapsulation by AAS. The copper(II) ion contents was estimated after encapsulation are only due to the presence of copper(II) complexes in nanopores of zeolite-Y. The Si and Al contents in Cu(II)–NaY and the zeolite complexes are almost in the same ratio as in the parent zeolite. The parent NaY zeolite has Si/Al molar ratio of 2.53 which corresponds to a unit cell formula $Na_{56}[(AlO_2)_{56}(SiO_2)_{136}]$. The unit cell formula of metal-exchanged zeolites shows a copper dispersion of 10.8 moles per unit cell $(Na_{33.8}Cu_{10.8}[(AlO_2)_{56}(SiO_2)_{136}] \cdot nH_2O)$. The analytical data of each complex indicates Cu:C:N molar ratios almost close to those calculated for the mononuclear structure. Elemental analysis and spectroscopic data's (Tables 1 and 2) show that all of the neat complexes have tetrahedral coordinated structure.

The absence of absorption at ca. 3400 cm^{-1} in the IR spectra of ligands shows that the free amino groups are absent, and the absence of a strong band at ca. 1670–1750 cm^{-1} shows the absence of ketonic groups. It confirms the elimination of water molecules and, as a result, cyclization takes places with formation of a macrocyclic ligand. In the IR spectra of $[H]_2-N_2O_2$ and $[CH_3]_2-N_2O_2$ (~1620 cm^{-1}), $[H]_2-N_4$ and $[CH_3]_2-N_4$ (~1615 cm^{-1}) and $[H]_2-N_2S_2$ and $[CH_3]_2-N_2S_2$ (~1605 cm^{-1}) a new band appears in all the ligands corresponding the $\upsilon(C=N)$ group. The IR spectra of these complexes show a moderate intensity absorption in the 1583–1597 cm^{-1} range attributed to the imine, $\upsilon(C=N)$ (Table 1). This moderate intensity absorption band is showing a shift to the lower side in the complexes, suggesting coordination through the nitrogen of the $\upsilon(C=N)$ group. The spectrum of ligand ($[H]_2-N_4$ and $[CH_3]_2-N_4$) shows a band at ~3310 cm^{-1} corresponding to $\upsilon(N-H)$ [17]. On complexation this band is shifted towards the lower side 3290 cm^{-1}. This indicates diversion of the electron cloud from the nitrogen of the imidazole or amino group, thus resulting in a lowering of the N–H stretching frequency [18]. Important IR bands of all complexes are recorded in Table 1.

The intensity of the peaks of encapsulated complex is, though, weak due to low concentration of the complex in zeolite, the IR spectrum of encapsulated complex is essentially similar to that of the free metal complex. However, a significant change in some important bands from free ligand has been noticed. For example, free ligand exhibits $\upsilon(C=N)$ stretch about 1620 cm^{-1}, while $[Cu([R]_2-N_2X_2)]^{2+}$–NaY and neat complex display this band at 1580 and 1595 cm^{-1}, respectively. This lower shift indicates the coordination of azomethine nitrogen to the copper

ion. Appearance of three to four bands in the low frequency region of 414–514 cm^{-1} suggests the coordination of phenolic oxygen and in addition to the azomethine nitrogen. The $[Cu([R]_2-N_2X_2)]^{2+}$–NaY exhibits bands at 1136, 1035, 960, 787 and 740 cm^{-1} due to zeolite framework. No significant broadening or shift of the structure-sensitive zeolite vibrations at 1130 cm^{-1} (due to asymmetric T–O stretch) on encapsulation indicates that there is no significant expansion of the zeolite cavity or dealumination during the encapsulation process. This, further indicates that structure of metal complex fit nicely within the cavity of the zeolite. Thus, IR and UV–vis data indicates the encapsulation of $[Cu([R]_2-N_2X_2)]^{2+}$–NaY in the zeolite nanocavity.

Electronic spectra of $[Cu([R]_2-N_2X_2)]^{2+}$ complexes were recorded in CHCl$_3$ solution over the range 400–700 nm (Table 1). The visible spectra of the $[Cu([R]_2-N_2X_2)]^{2+}$ complexes consists of a shoulders at ~485 nm and a maximum or a broad shoulder around ~557 nm, which can be assigned to the $dxz, yz \rightarrow dxy$ and $dx^2 - y^2 \rightarrow dxy$ transitions in D_2h symmetry [19]. The room temperature magnetic moments of $[Cu([R]_2-N_2X_2)]^{2+}$ (Table 1) fall in the range 1.74 μB which are typical for square-planar (D_4h) and tetrahedrally distorted (D_2h) mononuclear copper(II) complexes with a S = 1/2 spin state and did not indicate any antiferromagnetic coupling of spines at this temperature. The electronic spectra of Cu(II)–NaY does not show any absorption band above 300 nm, while spectrum of $[Cu([R]_2-N_2X_2)]^{2+}$–NaY displays one broad band at 315 nm, which is probably due to a symmetry forbidden ligand to metal charge transfer transition, similar to that observed in copper acetate [19] at 365 nm. A very weak but broad absorption at ~555 nm is also observed when highly concentrated sample in nujol mull was used to record the spectrum and this is due to d–d transition in the complex [19]. These data compare closely with that of pure complex $[Cu([R]_2-N_2X_2)](ClO_4)_2$ as well as of [Cu(salen)] and is indicative of a square-planer structure present in the nanocavity of the zeolite (Tables 1 and 2).

X-ray diffraction (XRD) patterns were recorded at 2θ values between 5° and 70° for NaY, Cu(II)–NaY, $[Cu([R]_2-N_2X_2)]^{2+}$–NaY and neat $[Cu([R]_2-N_2X_2)](ClO_4)_2$ complexes. XRD of these species indicate that the crystallinity of zeolite-Y is preserved during encapsulation of $[Cu([R]_2-N_2X_2)]$. Cu(II)–NaY and $[Cu([R]_2-N_2X_2)]^{2+}$–NaY exhibit essentially similar pattern to that of NaY, though, only slight change in the intensity of the bands was observed. This observation suggest that the supercage of NaY is able to accommodate the

Table 3

Surface area and pore volume data of 12-membered macrocyclic copper(II) complexes encapsulated in nanopores of zeolite Y

Sample	Surface area[a] ($m^2 g^{-1}$)	Pore volume[b] ($ml g^{-1}$)
NaY	545	0.31
Cu(II)–NaY	532	0.30
$[Cu([H]_2\text{-}N_4)]^{2+}$–NaY	485	0.27
$[Cu([CH_3]_2\text{-}N_4)]^{2+}$–NaY	481	0.26
$[Cu([H]_2\text{-}N_2O_2)]^{2+}$–NaY	488	0.26
$[Cu([CH_3]_2\text{-}N_2O_2)]^{2+}$–NaY	486	0.25
$[Cu([H]_2\text{-}N_2S_2)]^{2+}$–NaY	478	0.25
$[Cu([CH_3]_2\text{-}N_2S_2)]^{2+}$–NaY	475	0.24

[a] Surface area is the "monolayer equivalent area" calculated as explained in the Ref. [14,15].
[b] Calculated by the *t*-method.

$[Cu([R]_2\text{-}N_2X_2)]^{2+}$ without strain. A new band with a *d* value of 2.414 nm (at 2θ value of 37.4°) found in Cu(II)–NaY as well as $[Cu([R]_2\text{-}N_2X_2)]^{2+}$ is assigned due to copper(II) ions. As zeolite containing complex was carefully extracted with methanol to remove surface species and then stirred with NaCl to re-exchange uncomplexed copper(II), the existence of this band in the $[Cu([R]_2\text{-}N_2X_2)]^{2+}$–NaY suggest the presence of $[Cu([R]_2\text{-}N_2X_2)]^{2+}$ complex in the nanocavity. Location of other bands due to $[Cu([R]_2\text{-}N_2X_2)]^{2+}$ in $[Cu([R]_2\text{-}N_2X_2)]^{2+}$–NaY was not possible due to poor resolution of these bands in the XRD pattern. The encapsulation of the copper complexes inside the zeolite nanocavities is shown by scanning electron microscopy (SEM). Both X-ray diffraction and SEM indicated that zeolites with good crystallinity could be obtained during the encapsulation of copper(II) complexes by the FLM reaction.

The surface area and pore volume of the catalysts are shown in Table 3. The inclusion of 12-membered macrocyclic copper(II) complexes dramatically reduces the adsorption capacity and the surface area of the zeolite. It has been reported [20] that the BET surface area of X and Y zeolite containing phthalocyanine complexes are typically less than $100 m^2 g^{-1}$. The lowering of the nanopore volume and surface area indicate the presence of 12-membered macrocyclic copper(II) complexes

Fig. 1. Oxylation products distribution with neat complexes; $[Cu([R]_2\text{-}N_2X_2)](ClO_4)_2$ (reaction conditions: ethylbenzene = 0.105 g (1 mmol); catalyst = 0.004 mmol; 50% TBHP in ethylenedichloride = 0.42 ml; CH_3CN = 1 ml; temperature = 333 K).

within the nanocavities of the zeolites and not on the external surface.

The 12-membered macrocyclic copper(II) complexes exhibited good activity in the oxidation of ethylbenzene using TBHP (Table 4, Fig. 1). Blank reactions performed over NaY zeolite under identical conditions show only negligible conversion indicating that zeolite host is inactive for oxidation. Furthermore, TBHP alone is unable to oxidize the substrates in the absence of any catalyst. Also, no reaction occurred when aqueous hydrogen peroxide was used in place of TBHP, as the oxidant. In representative tests, zeolite complex was filtered out and the filtrate was analyzed for copper content using atomic absorption spectrophotometry. The absence of metal ions in solution phase indicates that no leaching of complexes has occurred during reaction, and that they are too intact in the pores. These observations suggest that the oxidations occur due to the catalytic nature of the encapsulated 12-membered macrocyclic complexes and no significant role is played by either the zeolite support or free complexes.

The zeolite-encapsulated complexes did not undergo any color change during the reaction and could be easily separated

Table 4

Oxidation of ethyl benzene with TBHP catalyzed by 12-membered macrocyclic copper(II) complexes[a]

Catalyst	Conversion (%)	Selectivity (%)		
		Acetophenone	*o-/p*-Hydroxyacetophenone	Others mainly[*]
$[Cu([H]_2\text{-}N_4)](ClO_4)$	62.7	88.4	8.3	3.3
$[Cu([H]_2\text{-}N_4)](ClO_4)$[b]	40.3	65.2	32.3	2.5
$[Cu([H]_2\text{-}N_4)](ClO_4)$[c]	60.1	80.5	11.9	7.6
$[Cu([H]_2\text{-}N_4)](ClO_4)$[d]	32.6	68.6	16.5	14.9
$[Cu([CH_3]_2\text{-}N_4)](ClO_4)$	56.8	83.5	9.1	7.4
$[Cu([H]_2\text{-}N_2O_2)](ClO_4)$	59.3	85.7	10.4	3.9
$[Cu([CH_3]_2\text{-}N_2O_2)](ClO_4)$	53.1	81.9	11.6	6.5
$[Cu([H]_2\text{-}N_2S_2)](ClO_4)$	41.6	60.3	27.1	12.6
$[Cu([CH_3]_2\text{-}N_2S_2)](ClO_4)$	37.7	52.6	27.5	19.9

[a] Reaction conditions: ethylbenzene = 0.105 g (1 mmol); catalyst = 0.004 mmol; 50% TBHP in ethylenedichloride = 0.42 ml; CH_3CN = 1 ml; temperature = 333 K.
[b] Catalyst = 0.002 mol.
[c] Catalyst = 0.006 mol.
[d] Catalyst = 0.008 mol.
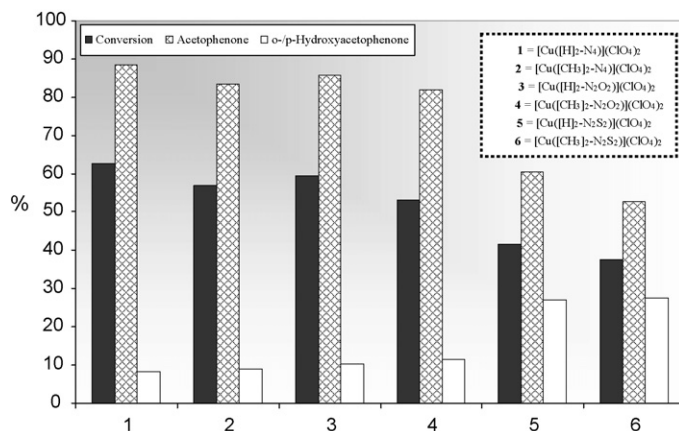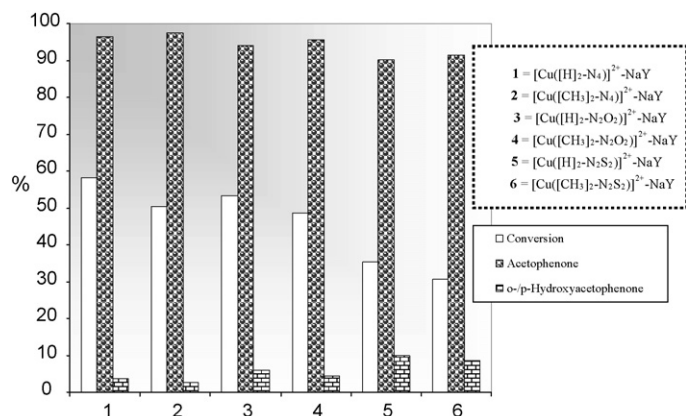[*] Other mainly products such as: benzaldehyde, benzoic acid and 1-phenylethanol.

Fig. 2. Oxylation products distribution with host–guest nanocatalyst (reaction conditions: ethylbenzene = 0.105 g (1 mmol); catalyst = 0.004 mmol; 50% TBHP in ethylenedichloride = 0.42 ml; CH$_3$CN = 1 ml; temperature = 333 K).

and reused many times. In contrast, the neat complexes, while they were active in the first cycle, were completely destroyed during the first run and changed color. The 12-membered macrocyclic ligands alone in the absence of metal were not catalytically active.

The effect of copper(II) complexes included in zeolite-Y were studied on the oxidation of ethylbenzene with TBHP in CH$_3$CN and the results are shown in Table 5. As shown in Fig. 2, the oxidation has occurred with the formation of acetophenone and o-/p-hydroxyacetophenone. The activity of Cu(II)–NaY catalyst has also been included in Table 5 to compare the effect of the ligand on the activity of catalyst. Increase of conversion percentage from 31.4 to 58.2% compared to Cu(II)-Y with [Cu([H]$_2$-N$_4$)]$^{2+}$–NaY indicates that the existence of ligand has increased the activity of catalyst by a factor of 1.85. From the results indicated in Tables 4 and 5 it is evident that acetophenone has been formed selectively in the presence of all catalysts though. The trend observed in Tables 4 and 5 can be explained by the donor ability of ligand available in the complex catalysts. As Wang et al. have pointed out recently, the key point in the

conversion of ethylbenzene to the products is the reduction of L-Cu^{3+} to L-Cu^{2+}. This reduction to L-Cu^{2+} is facilitated with the ligands available around the metal cation [21].

Comparing between "neat complexes" and host–guest nanocomposite materials as catalyst evidence that "neat complexes" gave higher conversion of ethylbenzene than their corresponding HGNM. For homogeneously catalyzed reactions, the termination of catalytic cycle may occur because of two factors, due to the formation of Cu–O–Cu species, which has poor catalytic activity, or due to the oxidative degradation of metal complexes (Tables 4 and 5 and Figs. 1 and 2). This was confirmed by taking the IR spectra of the solid after catalytic reaction. The IR spectra of these solids are very different from that of the IR spectra of the parent compounds. To improve the stability of the metal complex under the reaction conditions we have hydrogenised the complexes by preventing the catalytic species from dimerizing or aggregation, and to tune the selectivity of the reaction using the walls of the nanopores of the solid via steric effects.

Acetophenone is the major product; o-/p-hydroxyacetophenones and other products such as benzaldehyde are also formed in small quantities (Table 4). The type of the 12-membered macrocyclic ring and encapsulation affected the activity and product selectivity. Conversion for copper(II) complexes with different 12-membered macrocyclic ligands decreased in the order: [H]$_2$-N$_4$ > [H]$_2$-N$_2$O$_2$ > [CH$_3$]$_2$-N$_4$ > [CH$_3$]$_2$-N$_2$O$_2$ > [H]$_2$-N$_2$S$_2$ > [CH$_3$]$_2$-N$_2$S$_2$ (for "neat" and encapsulated complexes). Aromatic ring hydroxylation was more with [Cu([R]$_2$-N$_2$X$_2$)]$^{2+}$ complexes than [Cu([R]$_2$-N$_2$X$_2$)]$^{2+}$–NaY. Aromatic ring hydroxylation was less when the reactions were conducted using the encapsulated complexes (Table 5).

Homogeneous catalysts are more prone to deactivation by the isomerization of active centers, which is expected to be reduced by encapsulating them in zeolites. [Cu([H]$_2$-N$_4$)]$^{2+}$ was recycled for the oxidation of ethylbenzene with TBHP with a view to establish the effect of encapsulation on stability. The initial run has showed a conversion of 58.2% and it is only marginally

Table 5
Oxidation of ethylbenzene with TBHP catalyzed by host/guest nanocomposite materials[a]

Catalyst	Conversion (%)	Selectivity (%)		
		Acetophenone	o-/p-Hydroxyacetophenone	Others mainly product[e]
Cu(II)–NaY	31.4	62.7	3.2	40.5
[Cu([H]$_2$-N$_4$)]$^{2+}$–NaY	58.2	96.4	3.6	–
[Cu([H]$_2$-N$_4$)]$^{2+}$–NaY[b]	57.6	95.3	4.7	–
[Cu([H]$_2$-N$_4$)]$^{2+}$–NaY[c]	57.1	94.8	5.2	–
[Cu([H]$_2$-N$_4$)]$^{2+}$–NaY[d]	56.2	94.1	5.9	–
[Cu([CH$_3$]$_2$-N$_4$)]$^{2+}$–NaY	50.3	97.3	2.7	–
[Cu([H]$_2$-N$_2$O$_2$)]$^{2+}$–NaY	53.2	94.1	5.9	–
[Cu([CH$_3$]$_2$-N$_2$O$_2$)]$^{2+}$–NaY	48.6	95.6	4.4	–
[Cu([H]$_2$-N$_2$S$_2$)]$^{2+}$–NaY	35.4	90.2	9.8	2.3
[Cu([CH$_3$]$_2$-N$_2$S$_2$)]$^{2+}$–NaY	30.7	91.5	8.5	2.7

[a] Reaction conditions: ethylbenzene = 0.105 g (1 mmol); catalyst = 0.004 mmol; 50% TBHP in ethylenedichloride = 0.42 ml; CH$_3$CN = 1 ml; temperature = 333 K.
[b] First reuse.
[c] Second reuse.
[d] Third reuse.
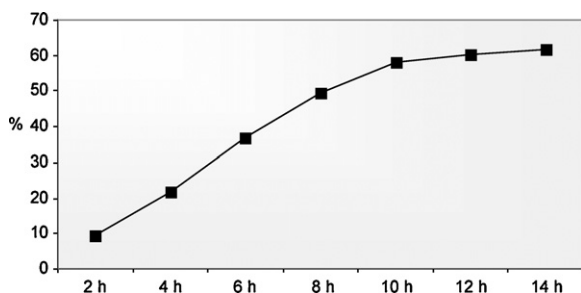[e] Other mainly products such as: benzaldehyde, benzoic acid and 1-phenylethanol.

Fig. 3. Effect of time on oxylation of ethylbenzene with TBHP (reaction conditions: ethylbenzene = 0.105 g (1 mmol); catalyst = 0.004 mmol; 50% TBHP in ethylenedichloride = 0.42 ml; CH_3CN = 1 ml; temperature = 333 K; catalyst: $[Cu([H]_2\text{-}N_4)]^{2+}$–NaY).
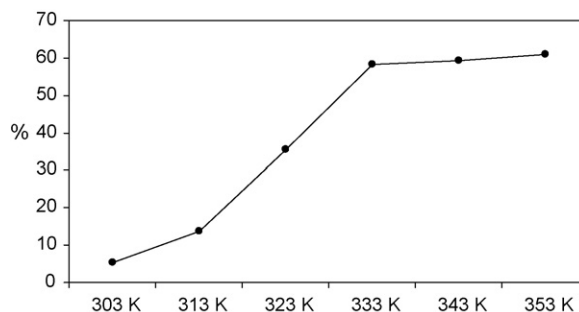

Fig. 4. Effect of temperature on oxylation of ethylbenzene (reaction conditions: ethylbenzene = 0.105 g (1 mmol); catalyst = 0.004 mmol; 50% TBHP in ethylenedichloride = 0.42 ml; CH_3CN = 1 ml; time = 10 h; catalyst: $[Cu([H]_2\text{-}N_4)]^{2+}$–NaY).

reduced to 57.6% on recycling the catalyst. These results indicate that $[Cu([R]_2\text{-}N_2X_2)]^{2+}$–NaY complex is almost stable to be recycled for the oxidation of ethylbenzene without much loss in activity. Thus, the encapsulation of complexes in zeolites is found to increase the life of the catalyst by reducing dimerization due to the restriction of internal framework structure. IR spectrum of the recycled sample is quite similar to that of fresh sample indicating little changes in the coordination of $[H]_2\text{-}N_4$ after the oxidation reactions.

The effect of time on the reactivity of catalysts is shown in Fig. 3. Fig. 3 shows that during 10 h, maximum conversion of starting material takes place with all catalyst systems. The effect of temperature on ethylbenzene conversion is studied at 303, 313, 323, 333, 343 and 353 K over $[Cu([R]_2\text{-}N_2X_2)]^{2+}$–NaY as catalyst. The results are presented in Fig. 4. Conversion increases with time and temperature (Figs. 3 and 4). The oxidation reaction was also tested at 373 K with TBHP as oxidant, but the conversion was found to be less, which might be attributed to

the decomposition of TBHP. The selectivity to acetophenone increases as the temperature raises from 303 to 333 K but at 373 K gradual decreases is observed; hence 333 K is the optimum temperature for the experiments.

TBHP is activated by coordinating with $[Cu([R]_2\text{-}N_2X_2)]^{2+}$–NaY. The activated distant oxygen of coordinated TBHP reacts with ethylbenzene to yield the above-mentioned products. α-Phenylethanol from ethylbenzene is produced by insertion of oxygen between carbon hydrogen bond of the –CH_2– group. Abstraction of an alcoholic OH hydrogen and the CH hydrogen by the activated *t*-butylhydroperoxide oxygen yields acetophenone. Similar abstraction of OH hydrogen of α-phenylethanol by the activated *t*-butylhydroperoxide yields benzaldehyde by forming methane. Similar to formation of α-phenylethanol, the –CHOH group of α-phenylethanol could also be acted upon by activated *t*-butylhydroperoxide to yield acetophenone. The oxidation products are evidenced through
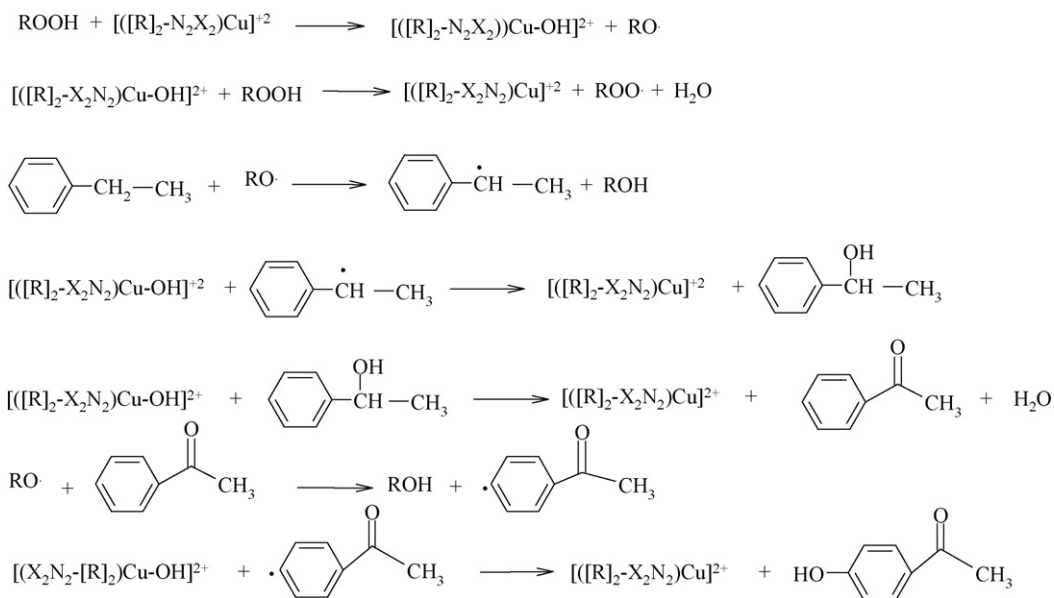
X = NH, O, S

R = H, CH$_3$

Scheme 3.

GC–MS analysis which indicates absence of α-phenylethanol after 10 h. So the main product obtained is found to be acetophenone (Scheme 3).

Acetophenone and benzophenone, are important intermediates for perfumes, drugs and pharmaceuticals. Production of these aromatic ketones by Friedel–Crafts acylation of aromatic compound by acid halide or acid anhydride, using a stoichiometric amount of anhydrous aluminum chloride or of a homogeneous acid catalyst, leads to the formation of a large volume of highly toxic and corrosive waste [22–24]. In the past, efforts have been made to produce aromatic ketones by oxidizing the methylene group attached to an aromatic ring using stoichiometric quantities of oxidizing agents, e.g., the oxidation of ethylbenzene to acetophenone by $KMnO_4$ [25], the oxidation of diphenylmethane to benzophenone by $KMnO_4$ [26], SeO_2 [27], or CrO_3 –SiO_2 [28], and the oxidation of alkylarenes by $KMnO_4$ supported on Mont-K10 [29]. However, in these stoichiometric oxidation reactions, the waste produced is very large and, moreover, the separation of reactants and products from the reaction mixture is difficult. Although the metal compound in this process is used in catalytic amounts, the reaction conditions are harsh, the product selectivity is poor, often corrosive promoters like bromide anions are used along with the catalyst, the separation of catalyst from the reaction mixture is difficult, the catalyst cannot be reused, and also a lot of tarry waste is produced. It is, therefore, of great practical interest to develop a more efficient, easily separable, reusable, and environmental-friendly catalyst for the production of aromatic ketones. Processes based on hydrocarbon oxidation particularly using molecular oxygen as an oxidizing agent are desirable [30]. Recently, $K_2Cr_2O_7$ supported on alumina [31] and Cr-MCM-41 or 48 [31], have been employed as incorporated catalysts for the oxidation by oxygen of ethylbenzene to acetophenone [32] and diphenylmethane to benzophenone [31]. However, the leaching of chromium from the catalyst during the reaction, the lengthy induction periods, and the rapid deactivation of the reused catalyst are serious problems [29–32]. For developing an environmental friendly/green process for the production of aromatic ketones, it is necessary to have a nontoxic and reusable solid catalyst, which shows high selectivity in the oxidation of ethylbenzene to acetophenone by TBHP and also without significant leaching of its components in the liquid reaction mixture. In this paper the results clearly suggest that $[Cu([H]_2-N_4)]^{2+}$–NaY efficiently catalyses conversion of ethylbenzene to acetophenone with 58.2% selectivity. More activity of $[R]_2$-N_2X_2 system has clearly arisen from the existence of electron donating ligand which facilitate the electron transfer rate, a process that has previously observed by us in other oxidation reactions [32]. All conversions efficiency with high selectivity obtained in this study is significantly higher than that obtained using metal containing porous and nonporous materials [22–32].

4. Conclusions

12-Membered macrocyclic ligands ($[R]_2$-N_2X_2; R = H, CH_3; X = NH, S, O) and their copper complexes have been encapsulated in the nanopores of zeolite Y. The resulting catalysts have been characterized by various spectroscopic (IR, DRS, UV–vis), techniques elemental analysis, etc. The "neat" and zeolite-Y-encapsulated copper(II) 12-membered macrocyclic complexes exhibit efficient catalytic activity in the oxidation of ethyl benzene using TBHP. C–H bond activation occurs at both the benzylic and aromatic ring carbon atoms. The latter is significant over the "neat" complexes in the homogeneous phase, while it is suppressed significantly in the case of the encapsulated complexes. The encapsulated complexes exhibit enhanced activity and selectivity in the oxidation reaction. These encapsulated systems offer structural integrity by having a uniform distribution of the metal complex in the nanopore structure of the support. The zeolite framework keeps the guest complexes dispersed and prevents their dimerization leading to the retention of catalytic activity. Future work on this system is expected to envisage its industrial applications for partial oxidation reactions.

Acknowledgment

References

[1] P.K. Dutta, J. Inclus, Phenom. Mol. Recognit. Chem. 21 (1995) 215.
[2] (a) P.-P. Knops-Gerrits, D.E. De Vos, F. Thibault-Starzyck, P.A. Jacobs, Nature 369 (1994) 543;
(b) I.F.J. Vankelecom, R.F. Parton, M.J.A. Casselman, J.B. Uytterhoeven, P.A. Jacobs, J. Catal. 163 (1996) 457.
[3] N. Herron, J. Coord. Chem. 19 (1988) 25.
[4] D.E. de Vos, P.P. Knops-Gerrits, D.L. Vanoppen, P.A. Jacobs, Supramol. Chem. 6 (1995) 49.
[5] P.P. Knops-Gerrits, D.E. de Vos, P.A. Jacobs, J. Mol. Catal. A 117 (1997) 57.
[6] M.R. Maurya, S.J.J. Titinchi, S. Chand, J. Mol. Catal. A: Chem. 214 (2004) 257.
[7] D. Chatterjee, H.C. Bajaj, A. Das, K. Bhatt, J. Mol. Catal. 92 (1994) L235.
[8] R. Raja, P. Ratnaswamy, J. Catal. 170 (1997) 244.
[9] M.L. Kantam, K.V.S. Ranganath, M. Sateesh, K.B.S. Kumar, B. Manoranjan, J. Mol. Catal. A: Chem. 225 (2005) 15.
[10] C. Hardacre, S.P. Katdare, D. Milroy, P. Nancarrow, D.W. Rooney, J.M. Thompson, J. Catal. 227 (2004) 44.
[11] V.R. Choudhary, S.K. Jana, N.S. Patil, S.K. Bhargava, Micropor. Mesopor. Mater. 57 (2003) 21.
[12] (a) E.F. Sousa-Aguiar, C.J.A. Mota, M.L.M. Valle, M.P. Silva, D.F. Silva, J. Mol. Catal. A: Chem. 104 (1996) 267;
(b) E.F. Sousa-Aguiar, M.L.M. Valle, M.P. Silva, D.F. Silva, Zeolites 15 (1995) 620.
[13] (a) M. Salavati-Niasari, J. Mol. Catal. A: Chem. 229 (2005) 159;
(b) M. Salavati-Niasari, Chem. Lett. 34 (2005) 244;
(c) M. Salavati-Niasari, J. Mol. Catal. A:Chem. 245 (2006) 192;
(d) M. Salavati-Niasari, J. Mol. Catal. A: Chem. 217 (2004) 87;
(e) M. Salavati-Niasari, Chem. Lett. 34 (2005) 1444.
[14] S.W. Wang, H. Everett, R.A.W. Haul, L. Moscou, R.A. Pierotti, J. Rouquerol, T. Siemieniewska, Pure Appl. Chem. 57 (1985) 603.
[15] A. Lineares-Solano, Textural characterization of porous carbons by physical adsorption of gases, in: J.L. Figueiredo, J.A. Moulijn (Eds.), Carbon and Coal Gasification, M. Nijhoff, M.A. Dordrecht, 1986, p. 137.
[16] C.R. Jacob, S.P. Varkey, P. Ratnasamy, Micropor. Mater. 22 (1998) 465, and references therein.
[17] (a) P.K. Singh, J.K. Koacher, J.P. Tondan, J. Inorg. Nucl. Chem 43 (1981) 1755;
(b) M. Salavati-Niasari, Inorg. Chem. Commun. 8 (2005) 174;

(c) M. Salavati-Niasari, Inorg. Chem. Commun. 7 (2004) 963;

(d) M. Salavati-Niasari, F. Davar, Inorg. Chem. Commun. 9 (2006) 263;

(e) M. Salavati-Niasari, F. Davar, Inorg. Chem. Commun. 9 (2006) 304;

(f) M. Salavati-Niasari, Micropor. Mesopor. Mater. 92 (2006) 173;

(g) M. Salavati-Niasari, Micropor. Mesopor. Mater. 95 (2006) 248.

[18] K. Nakamoto, Infrared Raman Spectra of Inorganic and Coordination Compounds, Wiley, New York, 1978.

[19] (a) A. Samyal, K.S. Kale, Ind. J. Chem. A 16A (1998) 46;

(b) A.H. Maki, B.R. McGarvey, J. Chem. Phys. 29 (1958) 35;

(c) I. Bertini, G. Canti, R. Grassi, A. Scozzafava, Inorg. Chem. 19 (1980) 2198.

[20] K.J. Balkus Jr., A.G. Gabrielov, J. Inclusion Phenom. Mol. Recognit. Chem. 21 (1995) 173.

[21] (a) M. Wang, C.J. Hao, Y.P. Wang, S.B. Li, J. Mol. Catal. A: Chem. 147 (1999) 173;

(b) M. Salavati-Niasari, Inorg. Chem. Commun. 9 (2006) 628;

(c) M. Salavati-Niasari, M. Bazarganipour, Catal. Commun. 7 (2006) 336;

(d) M. Salavati-Niasari, H. Banitaba, J. Mol. Catal. A: Chem. 201 (2003) 43;

(e) M. Salavati-Niasari, A. Amiri, Appl. Catal. A: Gen. 290 (2005) 46;

(f) M. Salavati-Niasari, P. Salemi, F. Davar, J. Mol. Catal. A: Chem. 238 (2005) 215.

[22] P.H. Groggins, R.H. Nagel, Ind. Eng. Chem. 26 (1934) 1313.

[23] H.J. Sanders, H.F. Keag, H.S. McCullough, Ind. Eng. Chem. 45 (1953) 2.

[24] G.A. Olah, Friedel–Crafts, Related Reactions, Wiley–Interscience, New York, 1963.

[25] C.F. Cullis, J.W. Ladbury, J. Chem. Soc. (1955) 2850.

[26] R. Gopalan, R.W. Sugumar, Indian J. Chem. 16A (1978) 198.

[27] N.D. Valechha, A. Pradhan, J. Indian Chem. Soc. 61 (1984) 909.

[28] S.D. Borkar, B.M. Khadilkar, Synth. Commun. 29 (1999) 4295.

[29] A. Shaabani, A. Bazgir, F. Teimouri, D.G. Lee, Tetrahedron Lett. 43 (2002) 5165;

(a) B.B. Wentzel, M.P.J. Donners, P.L. Alsters, M.C. Feiters, R.J.M. Nolte, Tetrahedron 56 (2000) 7797;

(b) V.F. Gaevskii, N.P. Evmenenko, Ukr. Khim. Zh. (Russ. Ed.) 48 (1982) 160;

(c) S.N. Vyas, S.R. Patwardhan, T.N. Pal, Indian Chem. Eng. 28 (1986) 44;

(d) G.B. Shul'pin, M.M. Kats, React. Kinet. Catal. Lett. 41 (1990) 239;

(e) J.H. Clark, S. Evans, J.R.L. Smith, Spec. Publ. -R. Soc. Chem. 216 (1998) 187.

[30] Y. Ishii, S. Sakaguchi, T. Iwahama, Adv. Synth. Catal. 343 (2001) 393, and references cited therein.

[31] J.H. Clark, A.P. Kybett, P. London, D.J. Macquarrie, K. Martin, J. Chem. Soc., Chem. Commun. (1989) 1355.

[32] (a) N.K. Mal, A.V. Ramaswamy, Appl. Catal. A: Gen. 143 (1996) 75;

(b) T. Radhika, S. Sugunan, Catal. Commun. 8 (2007) 150;

(c) H. Ma, J. Xu, Q. Zhang, H. Miao, W. Wu, Catal. Commun. 8 (2007) 27;

(d) S.S. Bhoware, S. Shylesh, K.R. Kamble, A.P. Singh, J. Mol. Catal. A: Chem. 255 (2006) 123;

(e) P.P. Toribio, J.M. Campos-Martin, J.L.G. Fierro, J. Mol. Catal. A: Chem. 227 (2005) 101;

(f) S. Vetrivel, A. Pandurangan, J. Mol. Catal. A: Chem. 217 (2004) 165;

(g) T.H. Bennur, D. Srinivas, S. Sivasanker, J. Mol. Catal. A: Chem. 207 (2004) 163;

(h) C. Guo, Q. Peng, Q. Liu, G. Jiang, J. Mol. Catal. A: Chem. 192 (2003) 295.